

Original Research

Sorption of Aqueous Methylene Blue, Cadmium and Lead onto Biochars Derived from Scrap Papers

Xuebin Xu¹, Xin Hu², Zhuhong Ding^{1,3*}, Bin Gao^{3**}

¹School of Environmental Science & Engineering, Nanjing Tech University, 30 Puzhu Southern Road, Nanjing 211816, P.R. China

²State Key Laboratory of Analytical Chemistry for Life Science, Center of Material Analysis and School of Chemistry and Chemical Engineering, Nanjing University, 22 Hankou Road, Nanjing 210093, P.R. China

³Agricultural & Biological Engineering Department, University of Florida, Gainesville, FL 32611, USA

Received: 8 December 2019

Accepted: 7 March 2020

Abstract

Biochars made from scrap newspaper and book paper (NPBx and BPBx, x represents pyrolysis temperature, °C) were characterized and used to remove methylene blue (MB), cadmium(Cd(II)) and lead (Pb(II)) from water solution. BPBx had higher yield, C content, and ash content and lower Ca content than NPBx made at the same temperature. Calcite and pyrophyllite were main minerals in NPBx and BPBx, respectively. Biochars made at higher temperature had higher pH_{pzc} values (6.9~11.0). The sorption kinetics of the three pollutants fit pseudo-second model well ($R^2 = 0.991\sim 0.999$). NPB300 and NPB450 had the largest Langmuir sorption capacity of about 23 mg g⁻¹ for MB, while BPB600 had the capacity of 19.5 mg g⁻¹. NPB600 had the largest Langmuir sorption capacity of 13.8 mg g⁻¹ for Cd(II) and 451 mg g⁻¹ for Pb(II). Column sorption capacities were 13.2 mg g⁻¹ (NPB300) and 9.46 mg g⁻¹ (NPB450) for MB and 7.39 mg g⁻¹ (NPB600) for Cd(II). De-ashed BPBx had greater sorption capacity for MB than pristine BPBx. Deposition caused by reaction with CaCO₃ was the main reason for Pb(II) sorption by NPB600. Scrap newspaper biochars derived at high temperatures were efficient sorbents for the removal of Pb(II).

Keywords: scrap paper biochar, batch sorption, column sorption, contaminant, precipitation

Introduction

As a form of pyrogenic carbon, plenty of studies have suggested that biochar has the preponderances of

carbon stabilization [1], renewable feedstock sources [2], relatively low cost [3], renewable energy resources [4], and excellent sorption ability [5]. As a consequence, it generally can be used as a novel, high-efficiency, and economical material for water treatment as well as soil remediation and carbon sequestration [6, 7]. Therefore, the preparation of biochar may be also a novel and low-cost technology for the recycling and reuse of waste biomass.

*e-mail: dzuhong@njtech.edu.cn

**e-mail: bg55@ufl.edu

The feedstock of biochar is comparatively far-ranging [8]. It has been demonstrated that feedstock type (i.e. fiber and mineral content) obviously influence the sorption ability of biochar [9, 10]. Generally, biochar prepared by fiber-rich biomass has higher carbon content and oxygen-containing functional groups compared to its biomass and shows superior affinity to some organic pollutants via hydrophobic interaction or hydrogen-bond interaction [11, 12]. However, mineral-rich biochar presents excellent combining capacity to some heavy metal contaminants by precipitation [13]. Hence, some fiber- and mineral-rich waste can be recycled for biochar and its values can be promoted. The main components of waste newspaper and book paper are cellulose, fillers/coating (e.g., calcium carbonate, kaolin, talcum powder, and so on), and adhesives (e.g., polyvinyl alcohol and carboxymethyl cellulose) [14]. In our previous study, mineral-rich waste-art-paper could be pyrolyzed to biochar product and the biochar was effective for Pb(II) removal from aqueous solution [15]. Therefore, further investigations should be carried out to develop scrap paper-based biochar as low-cost, high-efficient and environment-friendly adsorbent for wastewater treatment. Waste newspaper and book paper need to be deinked when making new paper, which makes the recycling process complicated and increases the cost of recycling. Otherwise, the wastewater and sludge produced from the deinking process may result in environmental pollution and also increase the cost of disposal [16, 17]. Therefore, the pyrolysis of waste newspaper and book to prepare biochar may be an environment-friendly and low-cost way for the preparation of a low-cost and high-efficient adsorbent for wastewater treatment. It is also a novel way for the disposal of waste paper.

Dyes are mainly used for coloring of food products, fabrics, textiles and leather products [18]. Some of them are harmful to human health when they are in excessive amounts [19]. In addition, the global emission of heavy metals has become a serious problem because of the toxicity of these metals toward living organisms [20]. Removal of these contaminants from sewage and wastewater has been a huge challenge for researchers. Biochar as a novel sorbent showed distinguished sorption performance to these pollutions [21]. Although most of the researches put more focus on batch experiment to examine pollution removal by biochar [22], fixed-bed column experiments were also carried on by some researchers [23].

The objective of this work is to develop high-efficient and low-cost adsorbents from scrap newspaper and book paper for the removal of aqueous MB, Cd(II) and Pb(II). The biochar samples derived from scrap newspaper and book paper rich of cellulose and minerals at 300, 450 and 600°C were subjected to elemental analyses, pH_{pzc} analyses, N₂ adsorption-desorption analyses, Fourier-Transform Infrared Spectroscopy analyses and X-Ray Diffraction analyses. Sorption efficiency was investigated using batch/column

sorption. Sorption mechanisms were discussed based on the sorption kinetics and isotherm sorption together with pH change and components of biochar.

Materials and Methods

Chemicals

Methylene blue (MB) stock solutions (2.0 g/L) were prepared by dissolving methylene blue with ultrapure water (18.3 MΩ·cm) from a Milli-Q Advantage A10 (Millipore, USA). Cd(II) and Pb(II) stock solutions (5.0 g/L) were prepared by dissolving Pb(NO₃)₂ and CdCl₂·2.5H₂O with the ultrapure water. All the reagents were purchased from Sinopharm Chemical Reagent Co., Ltd (Shanghai, P.R. China) and of analytical pure. All the labware were soaked in dilute nitric acid at least overnight, thoroughly flushed with tap water, and then with ultrapure water.

Production of Biochar

Scrap newspaper and book paper were collected from waste paper recycling bin and were snipped to fragments (about 2 cm×5 cm) using a scissor as feedstock. The fragments were tightly placed in a quartz tube, and then pyrolyzed in a tube furnace (OTF-1200X, USA) under N₂ atmosphere (10 psi). The pyrolysis was programmed to raise the internal biomass chamber temperature to 300, 450, and 600°C at a rate of 10°C/min and held at the peak temperature for 2 h before cooling to room temperature. The obtained biochars were also sieved with 60-mesh and 150 -mesh nylon sieves to obtain 0.106-0.25 mm fraction, marked as NPB_x and BPB_x (NPB and BPB refer to newspaper biochar and book paper biochar, respectively; “x” refer to the pyrolysis temperature), and stored in zip-lock polyethylene bags for further investigations. De-ashing of biochars was also performed to make de-ashed biochars to investigate the contribution of organic component in pristine biochar on the sorption capacity of MB. Briefly, 1mol L⁻¹ HCl and 10%(v/v) HF were add to react with 10g biochar sample in a polytetrafluoroethylene beaker for 24 h, then the supernatant was discarded after centrifugation. After being subjected to another two cycles of the reaction mentioned above, the residue was washed in a column for continuously waterlogged leaching with tap water and then distilled water. The washed residue was dried at 70°C in an oven to gain de-ashed biochar sample.

Characterization

Yield of biochar samples was calculated by mass difference of dry feedstock and the resultant product (biochar). Contents of C, H and N in biochar samples was determined using a CHN Elemental Analyzer (Carlo-Erba NA-1500). Mineral elements' content was

analyzed with an inductively coupled plasma optical emission spectrometer (ICP–OES, PerkinElmer Optima 5300 DV, USA) after ashing at 450°C for 4 h and aqua regia digestion. Points of zero charge (pHPZC) of the samples were measured by modified pH drift method [24, 25]. 0.200g biochar samples were degassed for 2 h under the temperature of 200°C, and then specific surface area of biochar samples was measured with a surface area analyzer (BET, ASAP2020, Micromeritics, Ltd., USA). Infrared spectrogram of biochar samples was measured by a Fourier transform infrared spectrometer (NEXUS870, NICOLET, USA) for characterizing the functional groups presented in the pristine and exhausted biochar. X-ray diffraction analysis for the samples was carried out with a powder X-ray diffraction photometer (XRD, CAD4/PC, Enraf Noius, NED).

Bath Sorption Experiments

In the batch experiment, 0.05 g biochar sample was mixed with 25 mL MB, Cd(II) or Pb(II) solutions in 50-mL plastic centrifuge tube. For the kinetics test, initial concentrations of MB and Cd(II) solutions were set up according to the pre-experiments and were set as 50 and 30 mg/L, respectively. Initial concentrations of Pb(II) was set as 30 mg/L for BPB300, 100 mg/L for BPB450, BPB600 and NPB300, and 1200 mg/L for NPB450 and NPB600. For the isotherms test, the initial concentration ranges of sorbates were set as 5–230 mg L⁻¹ for MB sorption, 1–44 mg L⁻¹ for Cd(II) sorption and 5–200 mg L⁻¹ or 500–2000 mg L⁻¹ for Pb. Initial pH value of MB solution was adjusted at 7.0±0.1 while Cd(II) solution and Pb(II) was adjusted at 5.5±0.1 by adding 0.1 mol/L (or 0.01 mol/L) NaOH and HNO₃ solutions. The plastic centrifuge tubes were sealed and agitated in a rotary shaker (120 r/min) at room temperature (25±2°C). At the end time of 1–1440 min, the mixtures were immediately centrifuged at 4000 rpm and filtered through 0.45-µm pore size nylon membranes. The final pH values of the filtrate

solutions were determined by pH meter. Cd(II), Pb(II) as well as released ions (i.e. Ca(II)) in the filtrates were determined using the ICP–OES. MB in the filtrates was determined by an ultraviolet and visible spectrophotometer at 663 nm and pH of 7.0. The adsorbing capacities were calculated as the difference between the initial and final solution concentrations of the sorbates.

Fixed-Bed Column Sorption Experiments

Fixed-bed column sorption experiments were set up according to the batch sorption experiments and our previous studies [22, 26]. Specifically, about 1.0 g of the tested biochar was wet-packed as an interlayer in an acrylic column measuring 1.5 cm in diameter and 5 cm in height. At each end of the column, acid-cleaned quartz sand (0.5–0.6 mm average size) was used to help distribute the flow. Polypropylene bolting cloth was stowed at juncture of sample and quartz sand to prevent possible loss of biochar sample. A peristaltic pump (Longer Pump, BT100-2J, China) was used at the influent of the column bottom to maintain an upward flow. Column effluent samples were collected every 2 min with a fraction collector (Shanghai Huxi Analysis Instrument Factor Co., Ltd, BS-100A, China) during the experiment and the concentrations of sorbates as well as freed ion (i.e. Ca(II)) were analyzed.

Results and Discussion

Basic Properties and Characterizations of the Biochars

The yield of NPBx decreased from 38.0% to 22.7%, and BPBx decreased from 47.0% to 32.5% with the increasing pyrolysis temperature from 300 to 600°C (Table 1). All the biochar samples were rich in carbon and the content of carbon ranged from 40.6 wt% to 50.5 wt%. An obvious decline of H, O, and N content

Table 1. Yield, specific surface area, elemental composition of C, H, O and N, and ash contents.

Biochars	SA (m ² .g ⁻¹)	Yield (%)	Elemental composition (wt%)						Ash (wt%)
			C	H	O ^a	N	H/C	(O+N)/C	
Newspaper			40.0	5.63	41.3	0.138	1.69	0.777	12.9
Book			39.3	5.94	46.4	0.0660	1.81	0.887	8.38
NPB300	5.05	38.0	42.9	2.90	25.1	0.180	0.811	0.442	28.9
NPB450	82.3	23.7	40.6	1.97	11.7	0.080	0.583	0.219	45.7
NPB600	225	22.7	43.6	1.50	11.8	0.050	0.413	0.204	43.0
BPB300	4.60	47.0	50.5	3.66	4.54	0.380	0.869	0.074	40.9
BPB450	46.9	36.7	47.9	2.00	1.71	0.110	0.501	0.029	52.3
BPB600	142	32.5	44.8	1.51	1.03	0.060	0.405	0.018	53.6

^a Calculated by mass difference assumed that the total mass of the samples was made up of the tested components only.

in biochar was observed with the increasing pyrolysis temperature, which indicated the degradation of organic components. Ratio of H/C decreased from 0.811 to 0.413 for NPBx and from 0.869 to 0.405 for BPBx, suggesting the strong carbonization and high aromaticity of the biochars at high pyrolysis temperature, which was consistent with the previous reports [6, 27]. Ratio of (N+O)/C also decreased from 0.442 to 0.204 in NPBx and from 0.074 to 0.018 in BPBx, reflecting a decreased polar-group content with the increasing pyrolysis temperature as the previous reports [28]. Ash content of biochars also increased with the increase of pyrolysis temperature (Table 1). Minerals contents of biochars indicated that NPBx samples were rich in Ca while BPBx samples were rich in Ca, Mg, and Al (Table S1 in the supplementary material).

The pH_{PZC} of the biochars were estimated by plotting the $\text{pH}_{\text{Initial}}$ against the pH_{Final} (Fig. S1a), with the sequence of BPB600 (11.0)>NPB600 (10.8)>NPB450 (10.2)>BPB450 (8.8)>NPB300 (8.3)>BPB300 (6.9). Generally, biochar shows positive surface charges and can attract anions when solution pH is lower than pH_{PZC} of the biochar, while show negative surface charges, favorite adsorption of cations, when solution pH is higher than pH_{PZC} of biochar [29]. According to the International Union of Pure and Applied Chemistry (IUPAC) classification [30], the tested biochars exhibited a typical type II isotherm, which suggests that the biochars were nonporous or macroporous adsorbents (Fig. S1b). The more gradual curvature of isotherm is an indication of a significant amount of overlap of monolayer coverage and the onset of multilayer adsorption [30]. The results show that the specific surface area of the resultant biochars increased with the increasing pyrolysis temperature (Table 1).

The FTIR spectra of the biochar samples in the wavenumber region from 500 to 4000 cm^{-1} are shown in Fig. S2a). The broadband at about 3396 cm^{-1} (O-H stretching vibrations of hydrogen bonded hydroxyl groups) [31] and serial adsorption at 1610 and 1699 cm^{-1} (C=O stretching vibrations) [32] in the biochars became weaken in biochars prepared at high pyrolysis temperature, which showed a decrease of oxygen-containing functional groups (similar to the result of element content). The infrared absorption band around 876, and 1429 cm^{-1} of waste newspaper biochars were assigned to the stretching vibration band of CO_3^{2-} [10]. The XRD spectra of the biochars are shown in Fig. S2b). The strong peak corresponding to calcite (CaCO_3 , PDF#05-0586) at 29.38° ($d = 3.04\text{\AA}$) in waste newspaper biochars were observed, which further confirmed that the main mineral in waste newspaper biochar was CaCO_3 . However, the strong peak at 9.51° ($d = 9.29\text{\AA}$) and 28.53° ($d = 3.13\text{\AA}$) corresponding to pyrophyllite ($\text{Al}_2\text{Si}_4\text{O}_{10}(\text{OH})_2$, PDF#46-1308) were observed in waste book paper biochars, suggesting that the main mineral in waste book paper biochar was pyrophyllite.

Batch Sorption Performance

Sorption Kinetics

The sorption capabilities of MB, Cd(II), and Pb(II) onto the biochars as a function of time are presented in Fig. 1. For MB sorption, the sorption process was very fast during the first 1.5 h, and then slowed down gradually. Overall, waste newspaper biochars showed

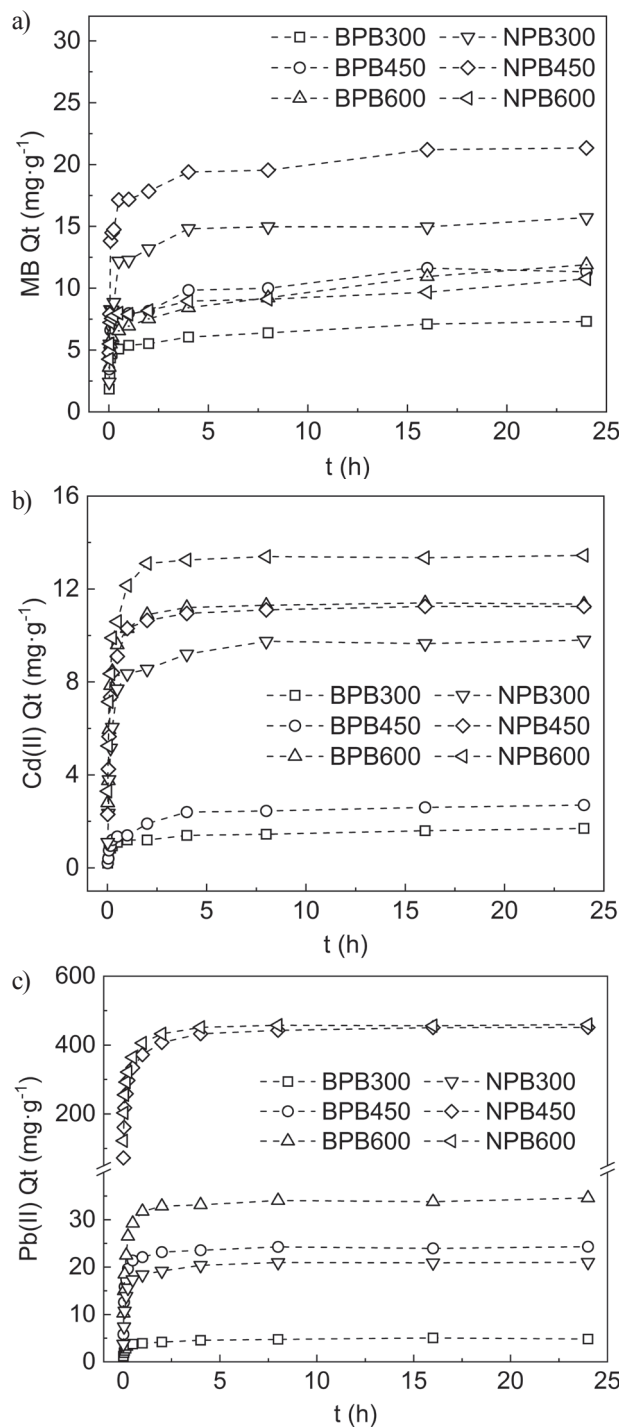


Fig. 1 Sorption kinetics of MB a), Cd(II) b) and Pb(II) c) onto biochars.

better MB sorption performance than waste book paper biochars. For Cd(II) and Pb(II) sorption, the initial sorption rate was rapid within the first 1 h, and then was followed by a slower reaction rate that gradually approached equilibrium within 3 h. In all biochars, NPB450 and NPB600 showed the highest sorption capacity to Pb(II) (above 400 mg/g). Simulations of the pseudo-second-order model fitted well with the experimental data with the correlation coefficients (R^2)

close to one (Table S2), suggesting that MB, Cd(II), and Pb(II) sorption onto resultant biochars could be mainly controlled by binuclear sorption processes [33].

Sorption Isotherms

Results showed that sorption capabilities of MB, Cd(II), and Pb(II) onto the biochar increased obviously and then reached a platform with the increasing equilibrium concentration (C_e) for all the resultant biochar samples (Fig. 2). The sorption performance of MB, Cd(II), and Pb(II) onto NPBx was generally higher than BPBx. In addition, the biochars pyrolyzed at high temperature showed better sorption performance to Cd(II) (13.8 and 12.4 mg g⁻¹ for NPB600 and BPB600, respectively) and Pb(II) (451 and 36.8 mg·g⁻¹ for NPB600 and BPB600, respectively) than that pyrolyzed at low temperature (Cd(II)/Pb(II): 10.0/21.0 mg·g⁻¹ for NPB300 and 1.83/5.32 mg·g⁻¹ for BPB300, respectively) (Table S3). According to correlation coefficients (R^2), the Langmuir model described the sorption data better ($R^2 = 0.982\sim 0.999$) than the Freundlich model ($R^2 = 0.402\sim 0.986$), which assumes monolayer sorption on the homogeneous surface (Table S3). The most eminent resultant biochars for sorption of MB, Cd(II), and Pb(II) were NPB300, BPB600, and NPB600, respectively. The Langmuir maximum sorption capacity of NPB600 for Pb(II) was 451 mg/g, which was much higher than that of other carbon-based sorbents including activated carbon reported in the literature (Table S4).

Column Sorption Performance

The column breakthrough curves of NPB300 and NPB450 columns, with initial MB concentration of 255 mg L⁻¹ and flow rate of 1.0 mL min⁻¹, both showed fast uptake of MB in initial stages and much slower uptake as saturation was reached at about 60 BV (Fig. 3a). The accumulated sorption amount of MB were 13.2 mg g⁻¹ (NPB300) and 9.46 mg g⁻¹ (NPB450) during the whole sorption process, respectively, which were lower than their Langmuir maximum sorption capacities of batch isotherm sorption (Table S3). The sorption breakthrough curve of Cd(II) in NPB600 column was conducted with initial Cd(II) concentration of 167 mg/L and flow rate of 1.0 mL/min (Fig. 3b). An obvious breakthrough point at about 25 BV was observed, and then the saturation stage began at about 60 BV. The accumulated sorption amount of Cd(II) was 7.39 mg g⁻¹ during the whole sorption process, which was lower than its Langmuir maximum sorption capacity of batch isotherm sorption (Table S3), consistent with the previously report [26, 34]. Roh et al. (2015) reported that the column sorption capacity for Cd(II) was slight higher than its Langmuir maximum sorption capacity of batch isotherm sorption at low flow rate and decreased significantly with the increasing flow rate from 0.25 to 1.0 mL/min at initial concentration of 20 mg L⁻¹ [35].

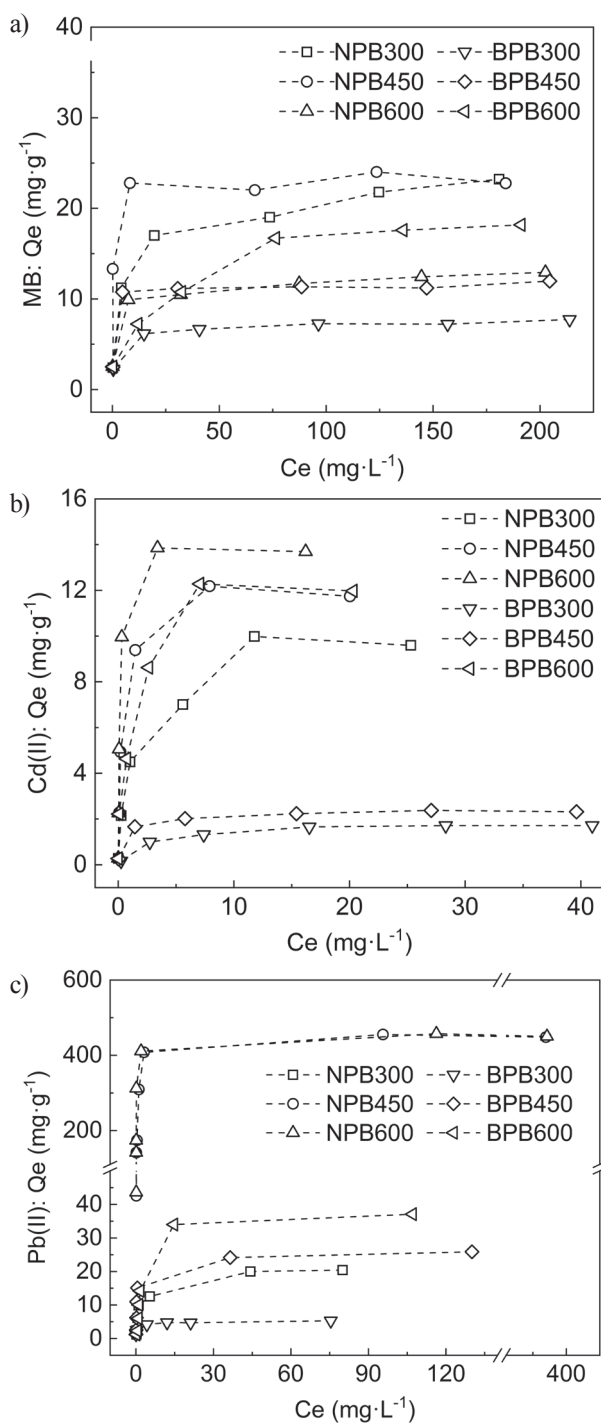


Fig. 2 Sorption isotherms of MB a), Cd(II) b) and c) Pb(II) onto biochars.

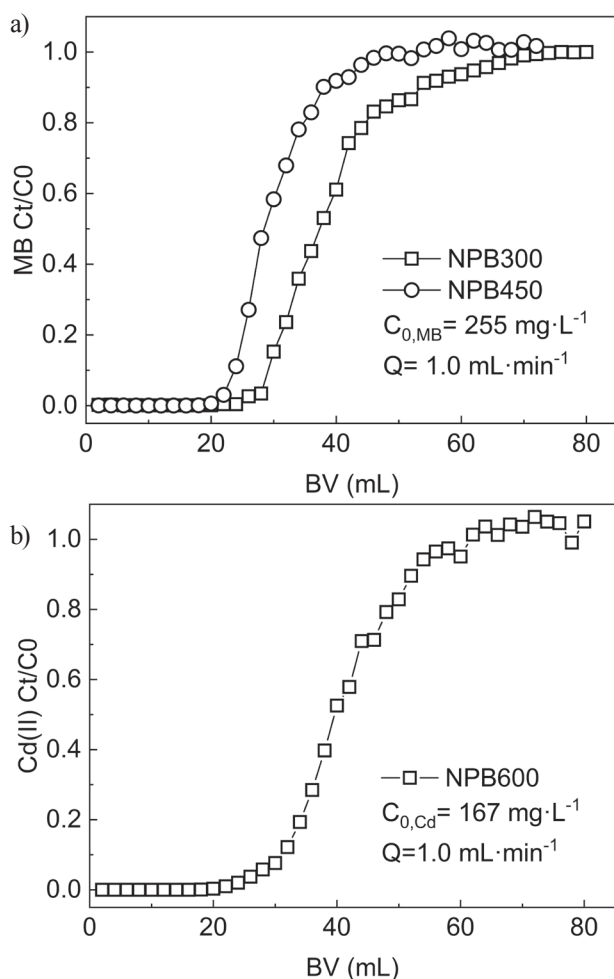


Fig. 3 MB a) and Cd(II) b) filtration in fixed-bed column packed with biochar.

Therefore, compared to the batch isotherm sorption, the lower sorption capacities of column sorption may be due to short residence time so that fine and ultrafine pores of the biochars might be not involved in the sorption. The parameters such as flow rate may be further optimized to improve sorption capacities. Moreover, physical sorption is generally faster than chemical sorption, so chemical sorption may play more important role on the sorption of MB and Cd in this study although they occur concurrently.

Sorption Mechanism

Effect of Solution pH and pH_{Hzc} of Biochar

pK_a of MB is 2.6 for methylamino and 11.2 for phenothiazinyl at 25°C, so MB is a cation in range of solution pH mentioned above. Biochars show positive charges when the solution pH is lower than pH_{Hzc} of biochars and negative charges when the pH above pH_{Hzc} [36]. In the sorption of MB by NPBx, final pH values were 8.08-8.30 (NPB300), 8.28-9.02 (NPB450) and 8.32-8.94 (NPB600) (Fig. S3a). The final pH values were all lower than pH_{Hzc} values of the three

NPBx biochars (Fig. S3a). It was not electrostatic attraction that contribute to the sorption of MB as the biochar surface was tending to be positively charged at pH lower than its pH_{Hzc}. In the sorption of MB by BPBx, final pH values were higher than the biochar pH_{Hzc} in the case of BPB300, while lower in the case of BPB600 and BPB600 (Fig S3a). It is suggested that the electrostatic attraction may contribute in the MB sorption onto BPB300, but more interactions involved MB sorption onto BPB450 and BPB600. Shi et al. (2014) reported that the main mechanism for the adsorption of MB onto anaerobic granular sludge-derived biochar included electrostatic interaction, ion exchange and surface complexation [37]. Yao et al. (2014) believed that electrostatic attraction was the main mechanism involving the adsorption of MB onto biochar in clay-biochar composite [38]. Lyu et al. (2018) pointed out that the sorption mechanisms of MB onto ball-milled biochar of different feedstock and pyrolysis temperature were π - π and electrostatic interactions (pH > PZC) [39]. So various mechanisms may be involved in the adsorption of MB onto biochar.

In the adsorption of Cd(II) onto NPBx and BPBx, final solution pH values were 7.28-7.75(NPB300), 7.65-8.34(NPB450), 8.08-8.87(NPB600), 6.84-7.66 (BPB300), 7.07-7.58 (BPB450), and 7.78-8.28 (BPB600) (Fig. S3b). Similar to the sorption of MB, the tested final pH values at equilibrium in NPBx treatments were lower than pH_{Hzc} values of the biochars, which implied that the sorption of Cd(II) by NPBx was other than electrostatic attraction. Electrostatic attraction may play a role in Cd(II) sorption by BPB300 as the final pH were higher than pH_{Hzc} value of BPB300. In adsorption of Pb(II), except final pH values of BPB300 treatment at low equilibrium Pb(II) concentration, the rest was all lower than pH_{Hzc} values of the adsorbents (Fig. S3c), which implied different sorption mechanism other than electrostatic attraction for Pb(II).

Effects of Biochar Components

As MB is an organic dye, its maximum sorption on de-ashed biochar was also investigated to find possible contribution of de-ashed component and ash component. For the sorption of MB by de-ashed NPBx, the Langmuir maximum sorption capacity was 8.10-11.4 mg·g⁻¹, much lower than the pristine biochar sorption (Fig. S4 and Table S3). For the sorption of MB by de-ashed BPBx, the Langmuir maximum sorption capacity was 12.2-24.1 mg·g⁻¹, much higher than the pristine biochar (Fig. S4 and Table S3). De-ashed component contributed greater than ash component in MB sorption by BPBx, while less important in MB sorption by NPBx. The different performance may be due to different elements contents, ash contents and minerals contents and types of BPBx and NPBx (Table 1 and Fig. S2b).

CaCO₃ was the main carbonate source of the waste newspaper biochar and the precipitation of heavy

metals by CO_3^{2-} may contribute to the sorption of the heavy metals [15]. Fig. S5 presents the XRD pattern of pristine, Cd(II)-laden, and Pb(II)-laden biochar. After Cd(II) sorption, the main mineral in Cd(II)-laden biochar was still CaCO_3 , as a result of the mediocre sorption performance to Cd(II). However, the XRD pattern of Pb(II)-laden biochar presented a series of new peaks which was attributed to cerussite (PbCO_3 , PDF#47-1734). This results indicated that one of the main mechanisms of Pb(II) sorption onto the resultant biochar is precipitation. Ca^{2+} released in the final solution after Cd(II) and Pb(II) sorption by NPB600 was recorded (Fig. S6). Molar ratio of sorbed-Cd(II)/Pb(II) and released-Ca increased and then then reached constant with the increasing of equilibrium concentrations of Cd(II)/Pb(II) (Fig. S6a, d). The molar ratio of sorbed-Cd(II)/Pb(II) and released-Ca stayed nearly constant between 60 min and 1440 min (Fig. S3b, e). It is obvious that Ca^{2+} released in the whole sorption process. Ca^{2+} release amount in column adsorption of Cd(II) (Fig. S6c) was also record. Ca^{2+} release amount was approximately 55mg/L at 20-30 BV where the breakthrough of Cd(II) began. Ca^{2+} release amount decreased sharply at 30-50 BV while Cd(II) concentration in the out fluent increased sharply. Then Ca^{2+} release amount and Cd(II) concentration in the out fluent reached nearly platforms after 60BV. These results implied that Ca may be replaced by Cd(II) during Cd(II) sorption by NPB600. At the end of the experiment, the accumulated Cd(II) adsorbed and Ca(II) released were 0.0658mmol and 0.0554mmol, respectively, with the Cd/Ca molar ratio of 1.19, which was close to that at maximum adsorption of Cd(II) in batch experiment. The ratios were all larger than 1, suggesting there may be specific sorption process other than reaction with CaCO_3 . In the research of Zhang et al, Cd was adsorbed mainly due to Cd- π interaction [40]. However, CaCO_3 might contribute to the sorption of Cd(II) in some extent, which was implied from the breakthrough curve of Cd(II) and release curve of Ca^{2+} . Ion exchange may be another mechanism of Pb(II)/Cd(II) sorption onto the resultant biochars.

Conclusion

Biochars made from scrap newspaper and book paper had different element contents, ash contents and mineral types, which may result in different sorption mechanisms. Biochars made at higher temperature had higher pH_{pzc} values. After 4h, the kinetics of the sorption of MB, Cd(II) and Pb(II) all nearly reached equilibrium and the data fit pseudo-second order model well. Newspaper biochar had better sorption performance for the three pollutants than book biochar made at the same temperature. Ash component and de-ashed component contributed differently in BPBx sorption and NPBx sorption of MB. Electrostatic attraction, ion exchange, surface complexation might

be involved in the sorption process of MB onto the resultant biochars. Surface precipitation, ion exchange, complexation/coordination with surface functional groups and π electrons were the possible mechanisms of Cd(II) sorption onto the resultant biochars. Precipitation caused by reaction with CaCO_3 and ion exchange were the main reason for Pb(II) sorption by NPB600, and NPB600 and NPB450 were efficient sorbents for removal of Pb(II). Therefore, pyrolysis of scrap paper to prepare high-efficient and low-cost adsorbents at higher pyrolysis temperatures (450-600°C) is a novel and reusing way for the disposal of scrap paper.

Acknowledgements

The work was supported by the National Key R&D Program of China (No. 2018YFC1800600), the National Natural Science Foundation of China (No. 21677075), and the Project of International Cooperation and Exchange of Nanjing Tech University (2017–2019). Ding Z. also thanks for the support of China Scholarship Council (CSC201808320034).

Conflict of Interest

The authors declare no conflict of interest.

Reference

1. WOOLF D., AMONETTE J.E., STREET-PERROTT F.A., LEHMANN J., JOSEPH S. Sustainable biochar to mitigate global climate change. *Nature Communications* **1**, 2010.
2. XIE T., REDDY K.R., WANG C.W., YARGICOGLU E., SPOKAS K. Characteristics and applications of biochar for environmental remediation: A Review. *Critical Reviews in Environmental Science and Technology* **45**, 939, 2015.
3. MOHAN D., SARSWAT A., OK Y.S., PITTMAN C.U. Organic and inorganic contaminants removal from water with biochar, a renewable, low cost and sustainable adsorbent – A critical review. *Bioresource Technology* **160**, 191, 2014.
4. KAMBO H.S., DUTTA A. A comparative review of biochar and hydrochar in terms of production, physico-chemical properties and applications. *Renewable & Sustainable Energy Reviews* **45**, 359, 2015.
5. AHMAD M., RAJAPAKSHA A.U., LIM J.E., ZHANG M., BOLAN N., MOHAN D., VITHANAGE M., LEE S.S., OK Y.S. Biochar as a sorbent for contaminant management in soil and water: a review. *Chemosphere* **99**, 19, 2014.
6. KEILUWEIT M., NICO P.S., JOHNSON M.G., KLEBER M. Dynamic molecular structure of plant biomass-derived black carbon (Biochar). *Environmental Science & Technology* **44**, 1247, 2010.
7. ZHANG M., GAO B., VARNOSFADERANI S., HEBARD A., YAO Y., INYANG M. Preparation and characterization of a novel magnetic biochar for arsenic removal. *Bioresource Technology* **130**, 457, 2013.
8. MOHAN D., KUMAR H., SARSWAT A., ALEXANDRE-FRANCO M., PITTMAN C.U. Cadmium and lead

- remediation using magnetic oak wood and oak bark fast pyrolysis bio-chars. *Chemical Engineering Journal* **236**, 513, **2014**.
9. SUN Y.N., GAO B., YAO Y., FANG J.N., ZHANG M., ZHOU Y.M., CHEN H., YANG L.Y. Effects of feedstock type, production method, and pyrolysis temperature on biochar and hydrochar properties. *Chemical Engineering Journal* **240**, 574, **2014**.
 10. XU X.Y., CAO X.D., ZHAO L. Comparison of rice husk- and dairy manure-derived biochars for simultaneously removing heavy metals from aqueous solutions: Role of mineral components in biochars. *Chemosphere* **92**, 955, **2013**.
 11. FANG Q.L., CHEN B.L., LIN Y.J., GUAN Y.T. Aromatic and Hydrophobic Surfaces of Wood-derived Biochar Enhance Perchlorate Adsorption via Hydrogen Bonding to Oxygen-containing Organic Groups. *Environmental Science & Technology* **48**, 279, **2014**.
 12. SUN K., KANG M.J., ZHANG Z.Y., JIN J., WANG Z.Y., PAN Z.Z., XU D.Y., WU F.C., XING B.S. Impact of deashing treatment on biochar structural properties and potential sorption mechanisms of phenanthrene. *Environmental Science & Technology* **47**, 11473, **2013**.
 13. INYANG M.I., GAO B., YAO Y., XUE Y., ZIMMERMAN A., MOSA A., PULLAMMANAPPALLIL P., OK Y.S., CAO X. A review of biochar as a low-cost adsorbent for aqueous heavy metal removal. *Critical Reviews in Environmental Science and Technology* **46**, 406, **2015**.
 14. PERNG Y.S., WANG E.I.C., CHANG C.P. Effect of co-binders for coating on the performance of fluorescent optical brightening agents. *Cellulose Chemistry and Technology* **49**, 209, **2015**.
 15. XU X., HU X., DING Z., CHEN Y., GAO B. Waste-art-paper biochar as an effective sorbent for recovery of aqueous Pb(II) into value-added PbO nanoparticles. *Chemical Engineering Journal* **308**, 863, **2017**.
 16. SIMSTICH B., BEIMFOHR C., HORN H. Lab scale experiments using a submerged MBR under thermophilic aerobic conditions for the treatment of paper mill deinking wastewater. *Bioresource Technology* **122**, 11, **2012**.
 17. LAHDENIEMI A., MAKELA M., DAHL O. Drying/fractionation of deinking sludge with a high-velocity cyclone. *Drying Technology* **31**, 378, **2013**.
 18. MAHMOUD D.K., SALLEH M.A.M., KARIM W.A.W.A., IDRIS A., ABIDIN Z.Z. Batch adsorption of basic dye using acid treated kenaf fibre char: Equilibrium, kinetic and thermodynamic studies. *Chemical Engineering Journal* **181**, 449, **2012**.
 19. SHI L., ZHANG G., WEI D., YAN T., XUE X., SHI S., WEI Q. Preparation and utilization of anaerobic granular sludge-based biochar for the adsorption of methylene blue from aqueous solutions. *Journal of Molecular Liquids* **198**, 334, **2014**.
 20. INYANG M., GAO B., YAO Y., XUE Y.W., ZIMMERMAN A.R., PULLAMMANAPPALLIL P., CAO X.D. Removal of heavy metals from aqueous solution by biochars derived from anaerobically digested biomass. *Bioresource Technology* **110**, 50, **2012**.
 21. KIM W.K., SHIM T., KIM Y.S., HYUN S., RYU C., PARK Y.K., JUNG J. Characterization of cadmium removal from aqueous solution by biochar produced from a giant Miscanthus at different pyrolytic temperatures. *Bioresource Technology* **138**, 266, **2013**.
 22. HU X., DING Z.H., ZIMMERMAN A.R., WANG S.S., GAO B. Batch and column sorption of arsenic onto iron-impregnated biochar synthesized through hydrolysis. *Water Research* **68**, 206, **2015**.
 23. HU X., DING Z., ZIMMERMAN A.R., WANG S., GAO B. Batch and column sorption of arsenic onto iron-impregnated biochar synthesized through hydrolysis. *Water Res* **68**, 206, **2015**.
 24. JIMENEZ-CEDILLO M.J., OLGUIN M.T., FALL C., COLIN-CRUZ A. As(III) and As(V) sorption on iron-modified non-pyrolyzed and pyrolyzed biomass from *Petroselinum crispum* (parsley). *J Environ Manage* **117**, 242, **2013**.
 25. FARIA P.C.C., ÓRFÃO J.J.M., PEREIRA M.F.R. Adsorption of anionic and cationic dyes on activated carbons with different surface chemistries. *Water Research* **38**, 2043, **2004**.
 26. DING Z., HU X., WAN Y., WANG S., GAO B. Removal of lead, copper, cadmium, zinc, and nickel from aqueous solutions by alkali-modified biochar: Batch and column tests. *Journal of Industrial and Engineering Chemistry* **33**, 239, **2016**.
 27. BOGUSZ A., OLESZCZUK P., DOBROWOLSKI R. Application of laboratory prepared and commercially available biochars to adsorption of cadmium, copper and zinc ions from water. *Bioresource Technology* **196**, 540, **2015**.
 28. CHEN Z., CHEN B., CHIOU C.T. Fast and slow rates of naphthalene sorption to biochars produced at different temperatures. *Environmental Science & Technology* **46**, 11104, **2012**.
 29. TAN X., LIU Y., ZENG G., XIN W., HU X., GU Y., YANG Z. Application of biochar for the removal of pollutants from aqueous solutions. *Chemosphere* **125**, 70, **2015**.
 30. THOMMES M., KANEKO K., NEIMARK A.V., OLIVIER J.P., RODRIGUEZREINOSO F., ROUQUEROL J., SING K.S.W. Physisorption of gases, with special reference to the evaluation of surface area and pore size distribution (IUPAC Technical Report). *Pure & Applied Chemistry* **87**, 25, **2015**.
 31. DARBY I., XU C.Y., WALLACE H.M., JOSEPH S., PACE B., BAI S.H. Short-term dynamics of carbon and nitrogen using compost, compost-biochar mixture and organo-mineral biochar. *Environmental Science & Pollution Research* **23**, 11267, **2016**.
 32. MUBARIK S., SAEED A., ATHAR M.M., IQBAL M. Characterization and mechanism of the adsorptive removal of 2,4,6-trichlorophenol by biochar prepared from sugarcane baggase. *Journal of Industrial & Engineering Chemistry* **33**, 115, **2015**.
 33. YAO Y., GAO B., INYANG M., ZIMMERMAN A.R., CAO X.D., PULLAMMANAPPALLIL P., YANG L.Y. Removal of phosphate from aqueous solution by biochar derived from anaerobically digested sugar beet tailings. *Journal of Hazardous Materials* **190**, 501, **2011**.
 34. WAN S., WU J., ZHOU S., WANG R., GAO B., HE F. Enhanced lead and cadmium removal using biochar-supported hydrated manganese oxide (HMO) nanoparticles: Behavior and mechanism. *Sci Total Environ* **616-617**, 1298, **2018**.
 35. ROH H., YU M.-R., YAKKALA K., KODURU J.R., YANG J.-K., CHANG Y.-Y. Removal studies of Cd(II) and explosive compounds using buffalo weed biochar-alginate beads. *Journal of Industrial and Engineering Chemistry* **26**, 226, **2015**.
 36. TAN X.F., LIU Y.G., ZENG G.M., WANG X., HU X.J., GU Y.L., YANG Z.Z. Application of biochar for the removal

- of pollutants from aqueous solutions. *Chemosphere* **125**, 70, **2015**.
37. SHI L., ZHANG G., WEI D., YAN T., XUE X.D., SHI S.S., WEI Q. Preparation and utilization of anaerobic granular sludge-based biochar for the adsorption of methylene blue from aqueous solutions. *J Mol Liq* **198**, 334, **2014**.
38. YAO Y., GAO B., FANG J.N., ZHANG M., CHEN H., ZHOU Y.M., CREAMER A.E., SUN Y.N., YANG L.Y. Characterization and environmental applications of clay-biochar composites. *Chem Eng J* **242**, 136, **2014**.
39. LYU H.H., GAO B., HE F., ZIMMERMAN A.R., DING C., TANG J.C., CRITTENDEN J.C. Experimental and modeling investigations of ball-milled biochar for the removal of aqueous methylene blue. *Chem Eng J* **335**, 110, **2018**.
40. ZHANG C., SHAN B., TANG W., ZHU Y. Comparison of cadmium and lead sorption by *Phyllostachys pubescens* biochar produced under a low-oxygen pyrolysis atmosphere. *Bioresource Technology* **238**, 352, **2017**.

Supplementary Materials

Removal of Methylene Blue, Cadmium and Lead from Water Solution with Biochars Pyrolyzed from Scrap Papers

Xuebin Xu¹, Xin Hu², Zhuhong Ding^{1,3*}, Yijun Chen², Bin Gao^{3**}

¹School of Environmental Science & Engineering, Nanjing Tech University, 30 Puzhu Southern Road, Nanjing 211816, P.R. China

²State Key Laboratory of Analytical Chemistry for Life Science, Center of Material Analysis and School of Chemistry and Chemical Engineering, 22 Hankou Road, Nanjing University, Nanjing 210093, P.R. China

³Agricultural & Biological Engineering Department, University of Florida, Gainesville, FL 32611, USA

Table S1. Mineral element contents (mg·g⁻¹) of the feedstocks and the resultant biochars.

	Mineral element content (mg·g ⁻¹)					
	K	Ca	Na	Mg	Al	Fe
Newspaper	0.0331	2.57	0.178	0.0950	1.83	0.0596
Book	0.0213	0.691	0.0517	0.415	0.945	0.0443
NPB300	0.536	62.2	3.00	2.65	11.6	4.42
NPB450	0.401	104	4.04	4.90	17.6	1.26
NPB600	0.562	109	4.34	4.98	22.0	1.19
BPB300	0.426	16.2	0.793	14.4	10.8	2.13
BPB450	0.248	6.68	0.371	12.8	7.39	1.23
BPB600	0.661	12.7	0.769	28.1	16.1	2.91

Table S2. Kinetic parameters of the pseudo-second-order and pseudo-first-order models for MB, Cd(II), and Pb(II) sorption onto biochars.

Sorbates	Biochar	Pseudo-first order kinetics $\ln(Q_e - Q_t) = \ln Q_e - k_1 t$			Pseudo-second order kinetics $t/Q_t = 1/(k_2 Q_e^2) + t/Q_e$		
		$Q_{e,cal}$	k_1	R^2	$Q_{e,cal}$	k_2	R^2
MB	BPB300	6.01	13.3	0.773	7.28	0.434	0.998
	BPB450	9.22	13.7	0.602	11.5	0.217	0.998
	BPB600	8.53	12.0	0.439	11.7	0.146	0.991
	NPB300	14.0	6.40	0.852	15.6	0.318	0.999
	NPB450	18.7	11.7	0.854	21.4	0.230	0.999
	NPB600	8.65	24.4	0.640	10.4	0.310	0.995

*e-mail: dzuhong@njtech.edu.cn

**e-mail: bg55@ufl.edu

Table S2. Continued.

Cd(II)	BPB300	1.39	6.10	0.823	1.68	1.46	0.997
	BPB450	2.37	1.85	0.852	2.72	0.741	0.999
	BPB600	10.8	8.20	0.939	11.4	1.07	0.999
	NPB300	9.14	4.90	0.964	9.84	0.580	0.999
	NPB450	10.6	7.99	0.940	11.3	0.902	0.999
	NPB600	12.7	8.09	0.897	13.5	0.866	0.999
Pb(II)	BPB300	4.41	7.91	0.852	4.90	1.41	0.999
	BPB450	22.8	13.2	0.917	24.3	0.566	0.999
	BPB600	32.4	9.53	0.891	34.5	0.306	0.999
	NPB300	19.7	8.04	0.947	21.1	0.434	0.999
	NPB450	414	6.62	0.898	454	0.0147	0.999
	NPB600	426	9.23	0.848	461	0.0230	0.999

Where $Q_{e,cal}$: equilibrium adsorption capacity calculated by pseudo-first or pseudo-second order kinetics ($\text{mg} \cdot \text{g}^{-1}$); k_1 : first-order apparent adsorption rate constants (h^{-1}); k_2 : second-order apparent adsorption rate constants ($\text{g} \cdot \text{mg}^{-1} \cdot \text{h}^{-1}$).

Table S3. Isotherm parameters for the Langmuir and Freundlich models for MB, Cd(II), and Pb(II) sorption onto biochars.

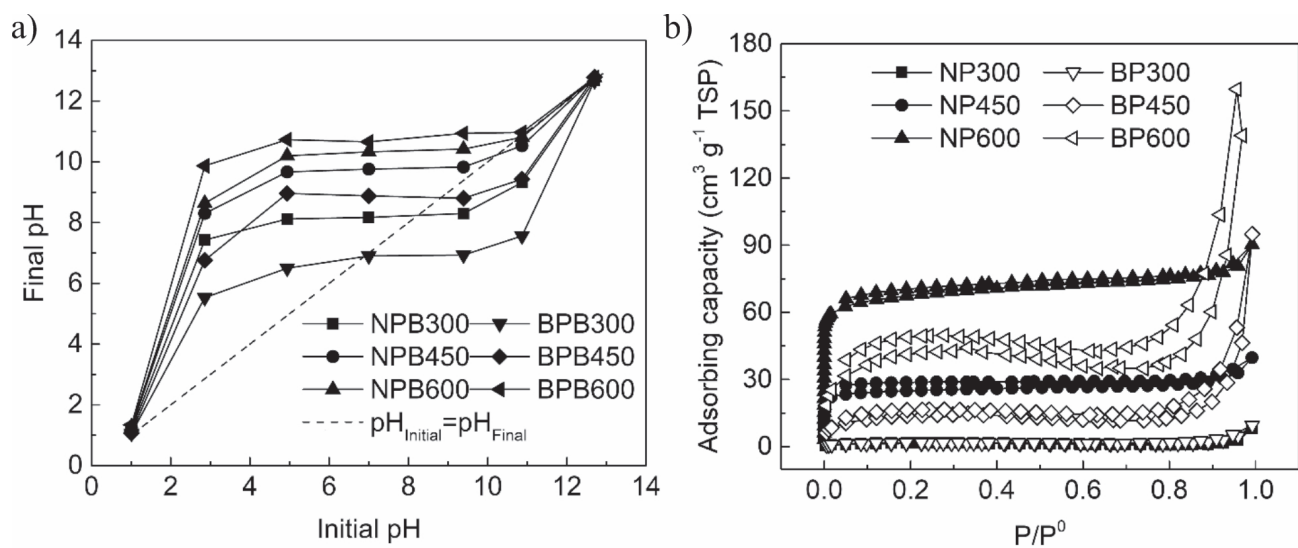
Sorbates	Biochar	Langmuir $Ce/Qe = 1/(K_L Q_m) + Ce/Q_m$			Freundlich $Qe = K_F \cdot Ce^{(1/n)}$		
		Q_m	K_L	R^2	K_F	n	R^2
MB	BPB300	7.69	0.230	0.998	2.98	5.15	0.929
	BPB450	11.8	0.523	0.998	4.62	4.77	0.765
	BPB600	19.5	0.0673	0.998	3.79	3.24	0.986
	NPB300	23.4	0.146	0.994	5.03	3.08	0.923
	NPB450	23.2	0.817	0.998	8.84	4.72	0.491
	NPB600	13.0	0.222	0.988	4.58	4.58	0.916
Cd(II)	BPB300	1.83	0.419	0.999	0.415	2.17	0.901
	BPB450	2.37	1.55	0.999	0.916	3.06	0.882
	BPB600	12.4	1.57	0.996	4.58	2.14	0.925
	NPB300	10.0	1.03	0.993	3.36	2.39	0.976
	NPB450	12.5	1.07	0.982	4.45	2.03	0.646
	NPB600	13.8	8.06	0.997	8.07	2.31	0.811
Pb(II)	BPB300	5.32	0.956	0.999	2.70	5.15	0.918
	BPB450	26.3	0.864	0.999	7.68	3.56	0.699
	BPB600	36.8	0.286	0.999	5.75	2.29	0.824
	NPB300	21.0	0.434	0.997	5.05	2.18	0.777
	NPB450	449	1.89	0.999	138	3.33	0.611
	NPB600	451	1.85	0.999	157	4.33	0.402

Where Q_m : maximum adsorption capacity ($\text{mg} \cdot \text{g}^{-1}$); K_L : Langmuir constant ($\text{L} \cdot \text{mg}^{-1}$); R^2 : coefficient of determination; K_F : affinity coefficient related to the bonding energy ($\text{mg}^{(1-1/n)} \cdot \text{L}^{1/n} \cdot \text{g}^{-1}$); n : the heterogeneity factor which represents the bond distribution.

Table S4. Comparison of lead sorption capacities of waste newspaper biochar with various biochars in previous studies.

Biochar	pH condition	Sorption capability	Sorption mechanism	References
<i>Phyllostachys pubescens</i> biochar	5.0±0.05	67.4 mg/g	Precipitation	[1]
Sewage sludge biochar	2.0-6.0	44.91 mg/g	NA	[2]
Magnetic sewage sludge biochar		249.00 mg/g	Electrostatic attraction, ion exchange, electrostatic surface complexation, inner-sphere complexation and co-precipitation	
Celery biochar	5.0	304 mg/g	Cation exchange, precipitation, and surface complexation	[3]
Banana peel based biochar	2-7	359 mg/g	Ions exchange and surface complexation	[4]
KMnO ₄ treated hickory wood biochar	2-7	153.1 mg/g	The surface functional groups and MnOx particles serve as the main adsorption sites for Pb(II)	[5]
Sugar cane bagasse biochar	2-6	86.96 mg/g	Supposed as a specific ion-exchange mechanism, and surface precipitation of metal ion hydroxides for both biochars	[6]
orange peel biochar		27.86mg/g		
Alkali-modified biochar	5.0	53.6 mg/g	NA	[7]
Functionalized graphene (GNS ^{PP6})	5.1	406.4 mg/g	NA	[8]
Activated carbon-alginate composite material	5	15.7 mg/g	NA	[9]
Lignin-grafted carbon nanotubes	2-7	221 mg/g	Complexation	[10]
Waste newspaper biochar	5.5	451 mg/g	Precipitation	This study

NA: not available.

Fig. S1. Point of zero charge (PZC) a) and N₂ adsorption-desorption isotherms b) of biochars.

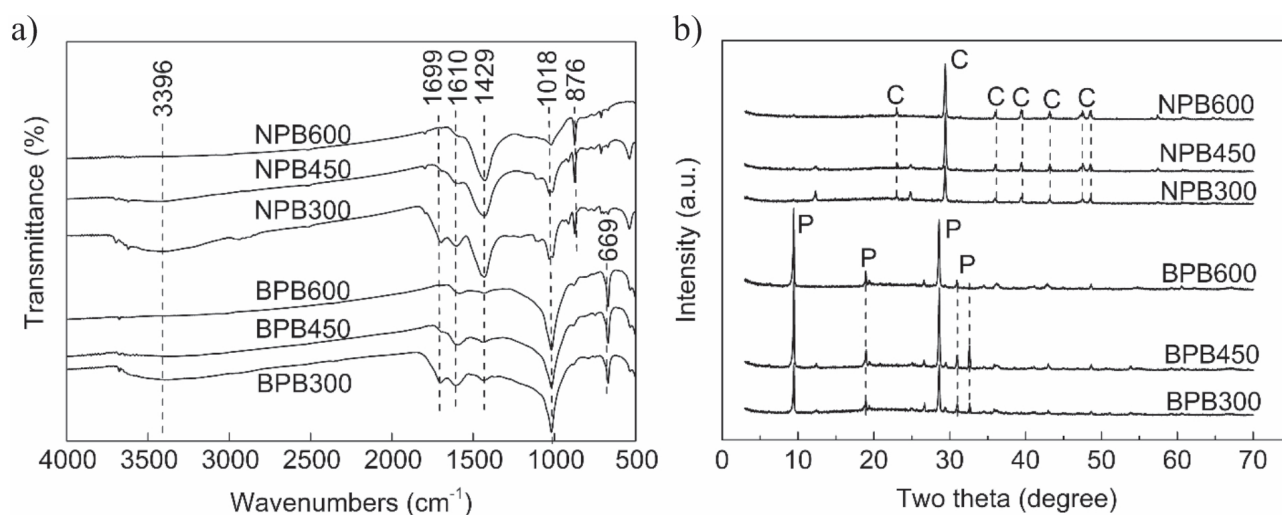


Fig. S2. FTIR spectra of bochars a) and XRD spectra of biochars b) (C refer to calcite, P refer to pyrophyllite).

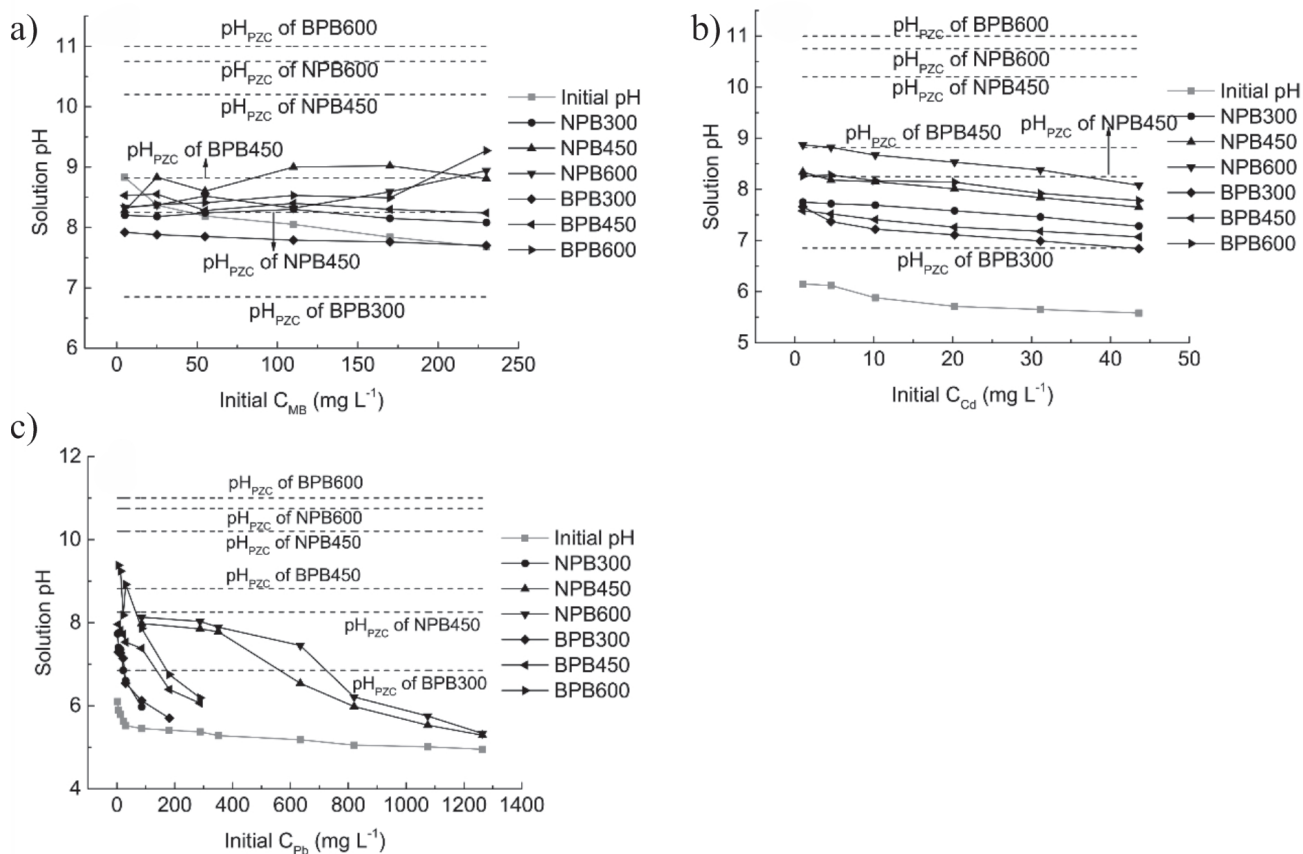


Fig. S3. Final pH values of the solutions in the sorption of MB a), Cd(II) b) and Pb(II) c).

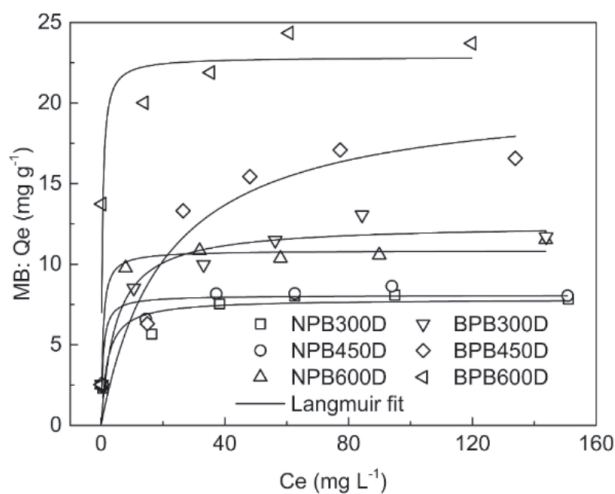


Fig. S4. MB adsorbed using de-ashed biochar.

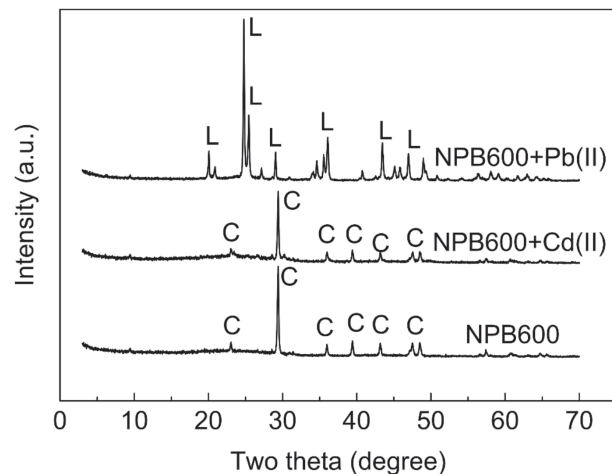


Fig. S5. XRD pattern of biochar after sorption (C refer to calcite, L refer to cerussite).

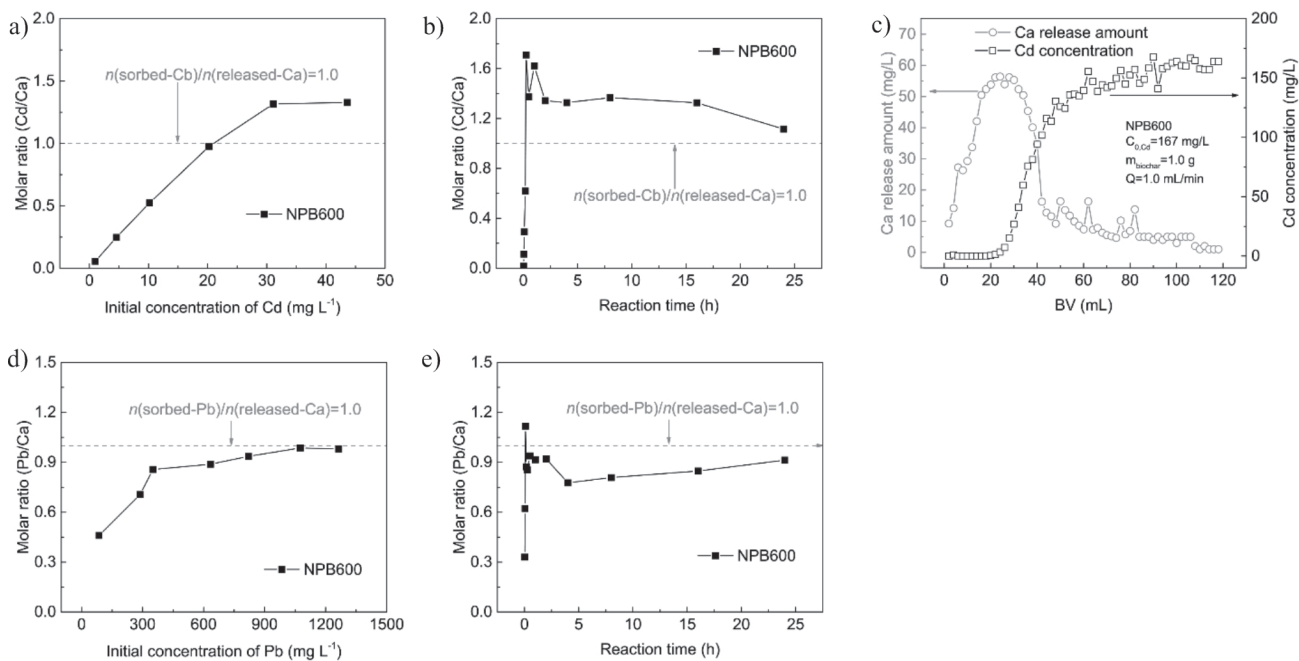


Fig. S6. Ca released during batch and column experiments. a) Molar ratio of sorbed-Cd and released-Ca as a function of initial Cd(II) concentration, b) Molar ratio of sorbed-Cd and released-Ca as a function of reaction time, c) Ca(II) release amount and Cd(II) concentration in solution during fixed-bed column sorption. f) Molar ratio of sorbed-Pb and released-Ca as a function of initial Pb(II) concentration, g) Molar ratio of sorbed-Pb and released-Ca as a function of reaction time.

References

- ZHANG C., SHAN B., TANG W., ZHU Y. Comparison of cadmium and lead sorption by *Phyllostachys pubescens* biochar produced under a low-oxygen pyrolysis atmosphere. *Bioresource Technology* **238**, 352, 2017.
- IFTHIKAR J., WANG J., WANG Q., WANG T., WANG H., KHAN A., JAWAD A., SUN T., JIAO X., CHEN Z. Highly efficient lead distribution by magnetic sewage sludge biochar: Sorption mechanisms and bench applications. *Bioresource Technology* **238**, 399, 2017.
- ZHANG T., ZHU X., SHI L., LI J., LI S., Lü J., LI Y. Efficient removal of lead from solution by celery-derived biochars rich in alkaline minerals. *Bioresource Technology* **235**, 185, 2017.
- ZHOU N., CHEN H., XI J., YAO D., ZHOU Z., TIAN Y., LU X. Biochars with excellent Pb(II) adsorption property produced from fresh and dehydrated banana peels via hydrothermal carbonization. *Bioresource Technology* **232**, 204, 2017.
- WANG H., GAO B., WANG S., FANG J., XUE Y., YANG K. Removal of Pb(II), Cu(II), and Cd(II) from aqueous solutions by biochar derived from KMnO_4 treated hickory wood. *Bioresource Technology* **197**, 356, 2015.

6. ABDELHAFEZ A.A., LI J. Removal of Pb(II) from aqueous solution by using biochars derived from sugar cane bagasse and orange peel. *Journal of the Taiwan Institute of Chemical Engineers* **61**, 367, **2016**.
7. DING Z., HU X., WAN Y., WANG S., GAO B. Removal of lead, copper, cadmium, zinc, and nickel from aqueous solutions by alkali-modified biochar: Batch and column tests. *Journal of Industrial and Engineering Chemistry* **33**, 239, **2016**.
8. DENG X., Lü L., LI H., LUO F. The adsorption properties of Pb(II) and Cd(II) on functionalized graphene prepared by electrolysis method. *Journal of Hazardous Materials* **183**, 923, **2010**.
9. CATALDO S., GIANGUZZA A., MILEA D., MURATORE N., PETTIGNANO A. Pb(II) adsorption by a novel activated carbon-alginate composite material. A kinetic and equilibrium study. *International Journal of Biological Macromolecules* **92**, 769, **2016**.
10. LI Z., CHEN J., GE Y. Removal of lead ion and oil droplet from aqueous solution by lignin-grafted carbon nanotubes. *Chemical Engineering Journal* **308**, 809, **2017**.